lubricants

MDPI

Article

Performance Evaluation and Lubrication Mechanism of Water-Based Nanolubricants Containing Nano-TiO_2 in Hot Steel Rolling

Hui Wu [1], Jingwei Zhao [1], Liang Luo [2], Shuiquan Huang [3], Lianzhou Wang [4], Suoquan Zhang [5], Sihai Jiao [5], Han Huang [3,*] and Zhengyi Jiang [1,*]

1 School of Mechanical, Materials, Mechatronic and Biomedical Engineering, University of Wollongong, Wollongong, NSW 2522, Australia; hwu@uow.edu.au (H.W.); jzhao@uow.edu.au (J.Z.)
2 Automotive Research Institute, Hefei University of Technology, Hefei 230009, China; Liang_LUO@hfut.edu.cn
3 School of Mechanical and Mining Engineering, The University of Queensland, Brisbane, QLD 4072, Australia; shuiquan.huang@uq.edu.au
4 School of Chemical Engineering, The University of Queensland, Brisbane, QLD 4072, Australia; l.wang@uq.edu.au
5 Baosteel Research Institute (R&D Centre), Baoshan Iron & Steel Co., Ltd., Shanghai 200431, China; zhangsuoquan@baosteel.com (S.Z.); shjiao@baosteel.com (S.J.)
* Correspondence: han.huang@uq.edu.au (H.H); jiang@uow.edu.au (Z.J.)

Received: 22 May 2018; Accepted: 29 June 2018; Published: 2 July 2018

Abstract: Hot rolling tests of a low-alloy steel were conducted at a rolling temperature of 850 °C under different lubrication conditions, including benchmarks (dry condition and water) and water-based nanolubricants containing different concentrations of nano-TiO_2 from 1.0 to 8.0 wt%. The effects of nanolubricants on rolling force, surface roughness, thickness of oxide scale, and microstructure were systematically investigated through varying nano-TiO_2 concentrations. The results show that the application of nanolubricants can decrease the rolling force, surface roughness and oxide scale thickness of rolled steels, and refine ferrite grains. In particular, the nanolubricant containing an optimal concentration (4.0 wt%) of nano-TiO_2 demonstrates the best lubrication performance, owing to the synergistic effect of lubricating film, rolling, polishing, and mending generated by nano-TiO_2.

Keywords: nano-TiO_2; water-based nanolubricant; hot rolling; grain refinement

1. Introduction

With a growing number of concerns about energy crisis and environmental pollution in modern society, "Green Manufacturing" or "Environmentally Conscious Manufacturing" and its sustainable development are becoming increasingly more important in the field of engineering applications [1]. Hot steel rolling, one of the most important manufacturing processes, has drawn considerable attention due to its huge energy consumption and pollutant emission. Previous studies have shown that the application of lubricants into hot steel rolling can lower the friction between work roll and workpiece [2–4], decrease rolling force [5,6], reduce thickness of oxide scale [6–8], increase roll service life [9,10], improve surface quality of rolled products [7,8,10], and refine grains in obtained microstructures [7,8]. These thus reduce energy consumption, increase yield and production efficiency, improve the mechanical properties of rolled steels, and bring about great economic benefits.

Nowadays, conventional neat oil and oil-in-water (O/W) emulsions have still been used most commonly in the research of hot steel rolling [2–4,6,10–14]. For examples, Matsubara et al. [4] investigated the relationship between the film thickness and the coefficient of friction (COF) value

in hot steel rolling by using neat lubricating oil instead of O/W emulsion on the work rolls in order to control the oil amount over a wide range. The results indicated that the COF decreased with the increase of oil film thickness up to around 0.2 μm, while it became constant even with a further increase of oil film thickness at 700 °C. The former was ascribed to the presence of dry lubrication area coupled with boundary lubrication area. The latter, in contrast, was affected by a combination of boundary and hydrodynamic lubrication, which separated the work roll and the workpiece from direct contact. Azushima et al. [2,3] developed a simulation testing machine for hot steel rolling to measure the COF and studied the lubrication mechanism using O/W emulsion with oil concentrations of 0–3.0 vol%. The results showed that the COF value decreased with the increase of oil concentration up to 1.0 vol%, while it remained constant when the oil concentration varied from 1.0 to 3.0 vol%, owing to mixed lubrication regime and hydrodynamic lubrication, respectively. In another case, it has been reported that 1:1000 O/W emulsion appeared to maximally decrease rolling force and torque in hot steel rolling at a rolling temperature of 850 °C, compared to other rolling conditions such as dry, hot forging oil, and 1:500 O/W emulsion [6]. Lenard et al. [12] also applied 1:1000 O/W emulsion to study the COF variation by means of inverse calculations at rolling temperatures of 850, 900, 950, and 1000 °C. They found that the COF increased when the rolling temperature decreased or when the pressures on the strip increased, and the COF tended to decrease when the rolling speed increased.

The application of lubricants that contain oil, however, inevitably causes environmental issues due to the inherent toxicity and nonbiodegradable nature of oil, especially when burnt and discharged during the hot steel rolling process [15]. In this regard, a type of environment-friendly lubricant with excellent lubricating performance is urgently needed to substitute conventional oil-containing lubricants. In recent years, the research trend on water-based lubricants added with nanoparticles (NPs) is continuously ascending due to their excellent tribological properties and promising potential in hot steel rolling, even though the relevant reports are still scarce [8,16–23]. For instance, Bao et al. [8] carried out hot steel rolling tests at temperatures of 750–950 °C using water-based lubricants containing SiO_2 NPs, and found that the use of as-prepared lubricants with the addition of 0.5 wt% nano-SiO_2 resulted in improved surface morphology, reduced oxide scale thickness, and refined grain size, compared to that of the base lubricant. The lubrication mechanisms were proposed to be the functions of micro-rolling, polishing, and self-repairing of SiO_2 NPs. Zhu et al. [19] performed experimental investigation on lubrication performance of water-based lubricants containing TiO_2 NPs during hot steel rolling at 950–750 °C. The results showed that the rolling force decreased significantly in each pass with the application of lubricant added with 2.0 wt% TiO_2, and the decreased extent of rolling force kept growing as the rolling temperature dropped continuously. The possible lubrication mechanism was supposed to be the formation of lubrication film on strip surface. The comprehensive lubrication effect of water-based nanolubricant on hot steel rolling together with the detailed lubrication mechanism and corresponding grain refinement mechanism, however, has not been fully understood.

In our previous study [22], the lubricating performance of water-based nanolubricants containing nano-TiO_2 applied in hot steel rolling has been analysed in terms of rolling force, surface roughness and oxide scale thickness of rolled steel with proposed lubrication mechanism. However, lubrication effect on surface microstructure and hardness and corresponding mechanism have not been examined until now. In the present work, comprehensive lubrication effects of water-based nanolubricant containing nano-TiO_2 on hot steel rolling were further systematically investigated including the effect on microstructure of rolled steel surface. Both the lubrication mechanism and the grain refinement mechanism were proposed based on advanced experimental techniques and detailed analyses.

2. Materials and Experimental Procedure

2.1. Materials

A low-alloy steel with yield stress of 345 MPa was used in this study. Its chemical compositions are listed in Table 1. The steel samples were machined to dimensions of 300 × 100 × 8 mm^3 with

tapered edges in order for an easy roll bite. Grinding and polishing were then performed on steel surfaces to generate a consistent surface roughness (R_a) of approximately 0.5 μm, which ensured the identical surface conditions. Before each hot rolling test, the samples were cleaned with acetone to remove the surface residuals such as debris and oil.

Table 1. Chemical compositions of the studied low-alloy steel (wt%).

C	Si	Mn	Mo	Ni	Cr	P	S	Nb + V + Ti
0.16	0.25	1.5	0.007	0.006	0.02	0.015	0.004	<0.02

The applied water-based nanolubricants containing nano-TiO_2 consisted of TiO_2 NPs, polyethyleneimine (PEI), glycerol and balanced water. PEI is a cationic polymer, which behaves as a surfactant in the water-based suspensions to improve the dispersibility of TiO_2 NPs in water. Glycerol is a colourless, odourless, and viscous liquid that is used to enhance the viscosity of suspensions. The detailed preparation process of the nanolubricants can be found in our previous study, and the lubricants exhibited excellent dispersibility and stability [21]. The chemical compositions of as-prepared nanolubricants in this study are outlined in Table 2. The dry condition and water were adopted as benchmarks in comparison to nanolubricants containing different concentrations of nano-TiO_2 varying from 1.0 to 8.0 wt%.

Table 2. Chemical compositions of applied lubricants.

Lubrication Type	Description
1	Dry condition
2	Water
3	1.0 wt% TiO_2 + 0.01 wt% PEI + 10.0 vol% glycerol + balance water
4	2.0 wt% TiO_2 + 0.02 wt% PEI + 10.0 vol% glycerol + balance water
5	4.0 wt% TiO_2 + 0.04 wt% PEI + 10.0 vol% glycerol + balance water
6	8.0 wt% TiO_2 + 0.08 wt% PEI + 10.0 vol% glycerol + balance water

2.2. Hot Rolling Tests

Hot rolling tests were carried out on a 2-high Hille 100 experimental rolling mill. The dimension of work rolls is Φ225 mm × 254 mm. Figure 1 shows the hot rolling process of the low-alloy steel, in which the steel samples were put into a high temperature electric resistance furnace and then heated up to 900 °C for a holding period of 30 min with nitrogen flowing inside at a rate of 15 L/min. Later on, the hot steel samples were rolled at 850 °C with a reduction of 30% and a rolling speed of 0.35 m/s under different lubrication conditions mentioned in Table 2, followed by an immediate cooling process in a sealed box full of nitrogen. The nitrogen used in hot rolling process aimed to refrain the steel samples from being oxidised with air, which aided the analysis of lubrication effect on steel oxidation. The lubricants were sprayed onto the pre-cleaned roll surface prior to each test until a saturated layer of lubrication film was formed. The saturation can be defined hereby in terms of the moment that the lubricants adhered onto roll surface began to drop down after formation of a uniform and compact lubrication film. It should be noted that the capacity of absorption of various lubricants on roll surface was inconsistent due to their different wettabilities. Two pieces of steel samples were tested under the same rolling and lubrication conditions to obtain an average value for a reasonable comparison of discrepant lubrication effectiveness.

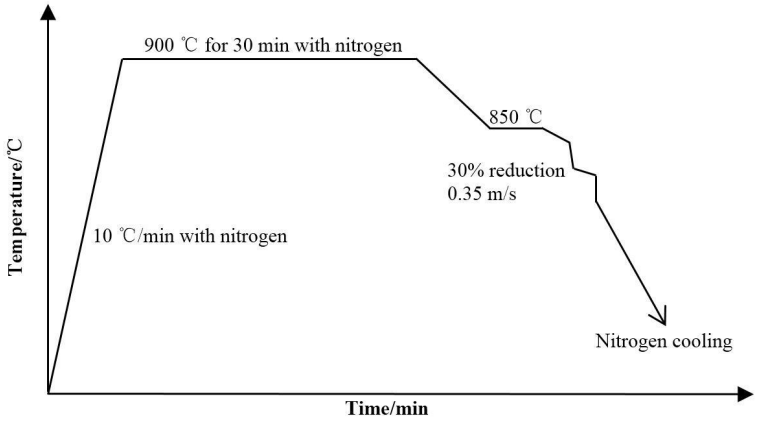

Figure 1. The procedure of hot rolling testing.

2.3. Characterisation Methodology

The rolling force during hot rolling was detected using two individual load cells assembled at the drive and operation sides in the rolling mill. The data acquisition was conducted by MATLAB xPC technology (2009b).

The surface roughness of rolled steels was measured by a KEYENCE VK-X100K three-dimensional (3D) Laser Scanning Microscope (Keyence Corporation, Osaka, Japan). The measurement of surface roughness was primarily focused on the centre of rolled steel surface by choosing five spots along the rolling direction to obtain average values.

The cross section of rolled steels along rolling direction was observed under a KEYENCE VK-X100K 3D Laser Scanning Microscope. Epoxy resin was mounted onto the rolled steel surface before cross-section observation in order to measure the oxide scale thickness. An FEI XT Nova NanoLab 200 (FEI Company, Hillsboro, OR, USA) which combines a dual beam of focused ion beam (FIB) and a high resolution field emission scanning electron microscope (FESEM) was used to characterise the cross-section morphology of rolled steel with further observation under a JEOL model JEM-ARM200F Transmission Electron Microscope (TEM, JEOL Ltd., Tokyo, Japan) coupled with an energy-dispersive spectrometer (EDS, JEOL Ltd., Tokyo, Japan). The dual beam FIB is equipped with a built-in platinum (Pt) gas injection system, which enables a thin layer of Pt deposition to form onto the top of region of interest (ROI). The selection of ROI was directed following the EDS mapping of Ti element obtained from FESEM.

The microstructure of rolled steels was observed under the 3D Laser Scanning Microscope, and the ferrite grain size obtained was statistically analysed based on a microstructural model reported by Luo et al. [24]. The thermal conductivity of applied lubricants was measured in air at an ambient temperature of 23.5 °C using a C-Therm TCi Thermal Conductivity Analyzer (C-Therm Technologies Ltd., Fredericton, NB, Canada). Each measurement was repeated 10 times to obtain an averaged value.

3. Results

3.1. Lubrication Effect on Rolling Force

Figure 2 shows the rolling force obtained at a rolling temperature of 850 °C under different lubrication conditions. It can be seen that the rolling force exhibited the highest value (605.2 KN) when no lubrication is applied. In contrast, the use of water and water-based nanolubricants resulted in a lower rolling force than that of the dry condition. With the increase of concentration of nano-TiO_2, the rolling force decreased gradually until it arrives at the lowest value of 564 KN (caused by the nanolubricant containing 4.0 wt% TiO_2). Further increase of nano-TiO_2 concentration to 8.0 wt% led

to slightly higher rolling force instead. In this case, 4.0 wt% TiO_2 acting as an optimal concentration contributes to lowering the rolling force by 6.8%, compared to that of the dry condition.

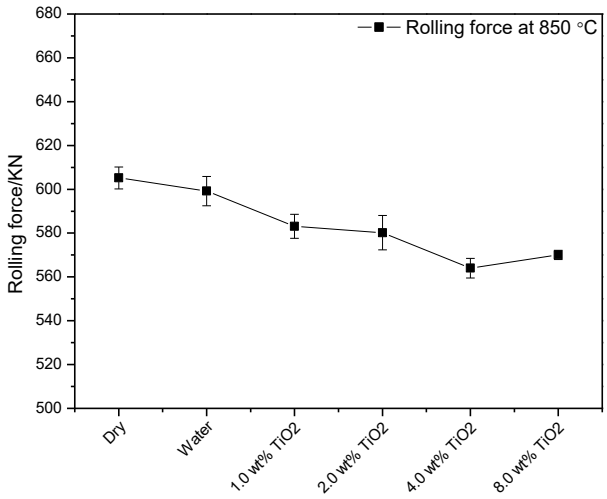

Figure 2. Rolling force obtained at 850 °C under different lubrication conditions.

3.2. Lubrication Effect on Surface Roughness

Figure 3 shows the 3D profiles of surface morphologies of rolled steels at 850 °C under different lubrication conditions. It is seen from Figure 3a that the rolled surface with no lubrication displays severe undulations with considerable peaks and valleys, indicating the roughest surface among all of the rolled surfaces. Similarly, water lubrication brings forth comparable surface morphology to that of dry condition with slightly better flatness, as shown in Figure 3b. Instead of these relatively rough surfaces produced, however, the application of nanolubricant was inclined to flatten the surface with increasingly higher concentrations of nano-TiO_2 with up to 4.0 wt% added into water before it yielded the smoothest rolled surface (Figure 3e). However, a higher concentration of 8.0 wt% aggravated the surface condition (Figure 3f).

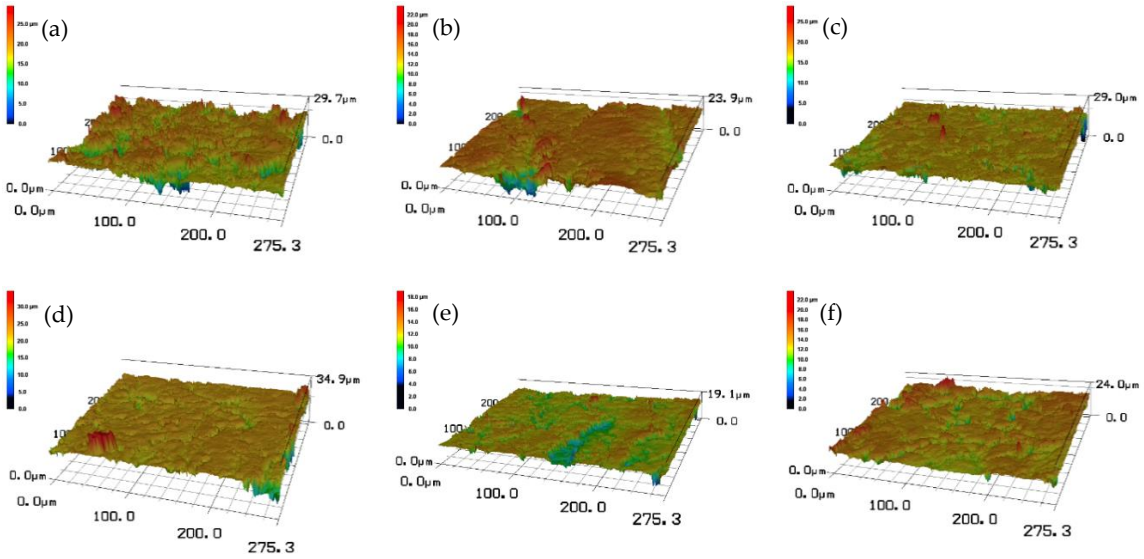

Figure 3. Three-dimensional (3D) profiles of surface morphologies of rolled steels at 850 °C under different lubrication conditions of (**a**) dry, (**b**) water, (**c**) 1.0 wt% TiO_2, (**d**) 2.0 wt% TiO_2, (**e**) 4.0 wt% TiO_2 and (**f**) 8.0 wt% TiO_2.

The effect of lubrication conditions on surface roughness of the rolled steels at 850 °C is shown in Figure 4. The varying trend of surface roughness corresponds to the surface morphologies displayed in Figure 3, suggesting that the optimal concentration of nano-TiO_2 in water-based nanolubricants to improve the surface quality of rolled steel is 4.0 wt%.

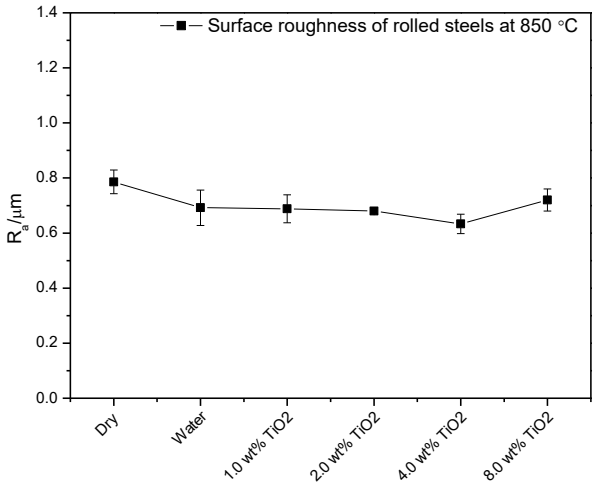

Figure 4. Surface roughness of rolled steels at 850 °C under different lubrication conditions.

3.3. Lubrication Effect on Oxide Scale

The morphologies of the oxide scales formed on the rolled steel at 850 °C under different lubrication conditions along cross sections are summarised in Figure 5. It can be found that the thickness of oxide scales formed under dry conditions, and water was apparently reduced when water-based nanolubricants were applied, and the reduction of scale thickness was in proportion to the increase of nano-TiO_2 concentration from 1.0 to 4.0 wt%. When the nano-TiO_2 concentration continued to increase to 8.0 wt%, conversely, the scale thickness became thicker than that caused by nanolubricant containing 4.0 wt% TiO_2. The statistical thickness values of oxide scale formed on rolled steel surface at 850 °C are shown in Figure 6. Most importantly, the oxide scale thickness formed under dry condition could be maximally reduced by 43.8% under nanolubricant containing 4.0 wt% TiO_2.

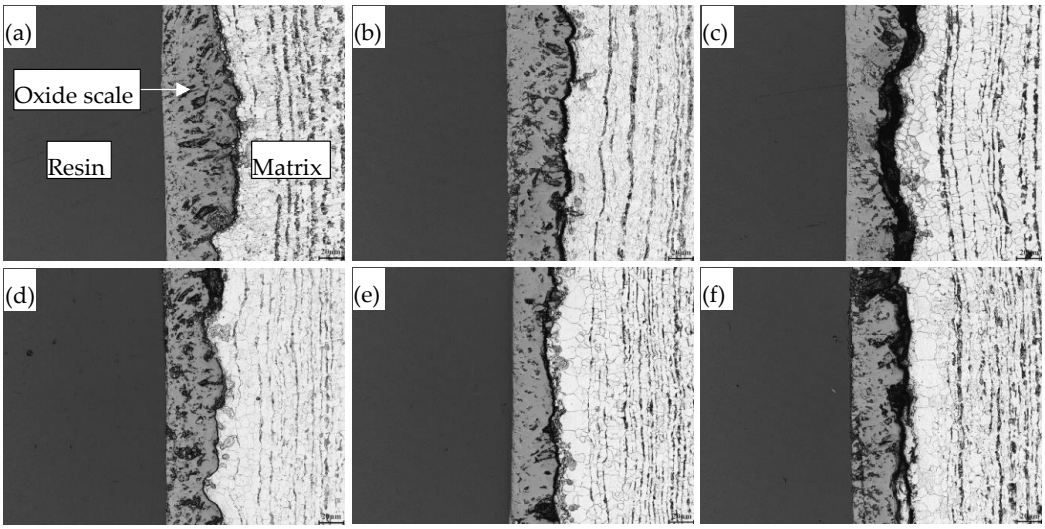

Figure 5. Morphologies of oxide scales formed at 850 °C under lubrication conditions of (**a**) dry; (**b**) water; (**c**) 1.0 wt% TiO_2; (**d**) 2.0 wt% TiO_2; (**e**) 4.0 wt% TiO_2; and (**f**) 8.0 wt% TiO_2.

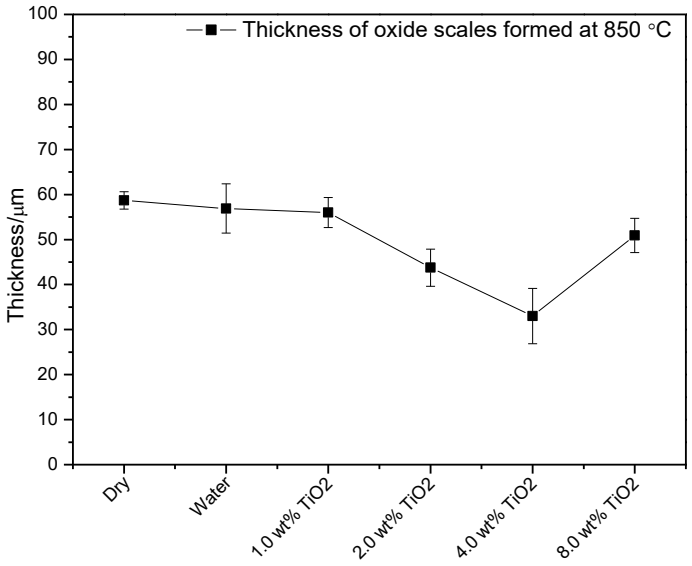

Figure 6. Thickness of oxide scales formed at 850 °C under different lubrication conditions.

3.4. Lubrication Effect on Surface Microstructure and Hardness

Figure 7 demonstrates the surface microstructures of rolled steels at 850 °C under different lubrication conditions. It can be seen that the microstructure primarily consisted of abundant polygonal ferrite (gray zones) and a small amount of pearlite (black zones). There is no significant change on the pearlite formed in terms of its amount and size. Nevertheless, it is of great interest that the ferrite grains obtained under dry condition and water lubrication can be refined to a large extent under nanolubrication, and especially nanolubricant containing 4.0 wt% TiO_2 leads to the finest ferrite grains, as shown in Figure 7e. The variation trend of grain refinement was consistent with those of the rolling force (Figure 2), surface roughness (Figure 4), and thickness of oxide scale (Figure 6). This clearly indicates that the water-based nanolubricant containing 4.0 wt% TiO_2 revealed the best lubrication effects on hot steel rolling at a rolling temperature of 850 °C.

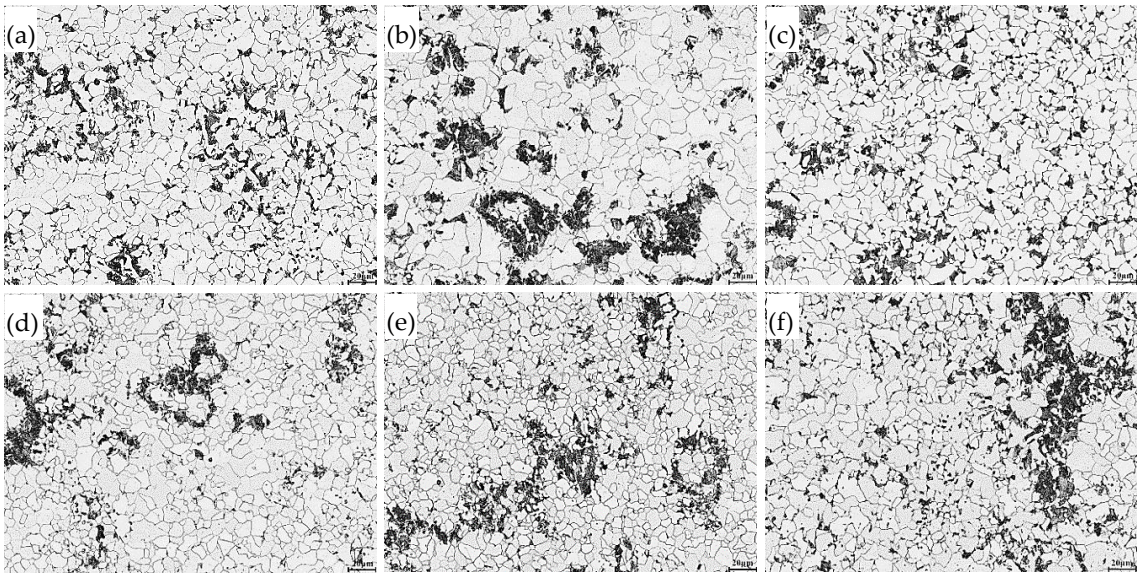

Figure 7. Surface microstructures of rolled steels at 850 °C under different lubrication conditions of (**a**) dry; (**b**) water; (**c**) 1.0 wt% TiO_2; (**d**) 2.0 wt% TiO_2; (**e**) 4.0 wt% TiO_2 and (**f**) 8.0 wt% TiO_2.

The size distributions of ferrite grains are statistically shown in Figure 8, corresponding to the microstructures shown in Figure 7. The statistical method of grain size can be referred to that reported by Luo et al. [24], in which the grain shape was equivalent to be spherical. It can be clearly seen that the majority of ferrite grains had diameters in the range of 7–13 μm under lubrication conditions of dry and water. In contrast, the grain size tended to become smaller and smaller with the application of nanolubricants by increasing nano-TiO_2 concentration from 1.0 to 4.0 wt%. A further increase of nano-TiO_2 concentration to 8.0 wt%, however, resulted in a slightly coarser grain size. The averaged grain size of ferrite obtained at 850 °C under different lubrication conditions is shown in Figure 9. It was found that dry condition triggered the coarsest averaged grain size of around 11.1 μm, which was refined to approximately 5.5 μm in diameter by using nanolubricant containing 4.0 wt% TiO_2. The variation trend of averaged grain size was in line with that of surface hardness, showing that the finer the grain size is, the higher surface hardness would be. To sum up, the grain size was refined by 50.5%, leading to an improved surface hardness by 4.9%.

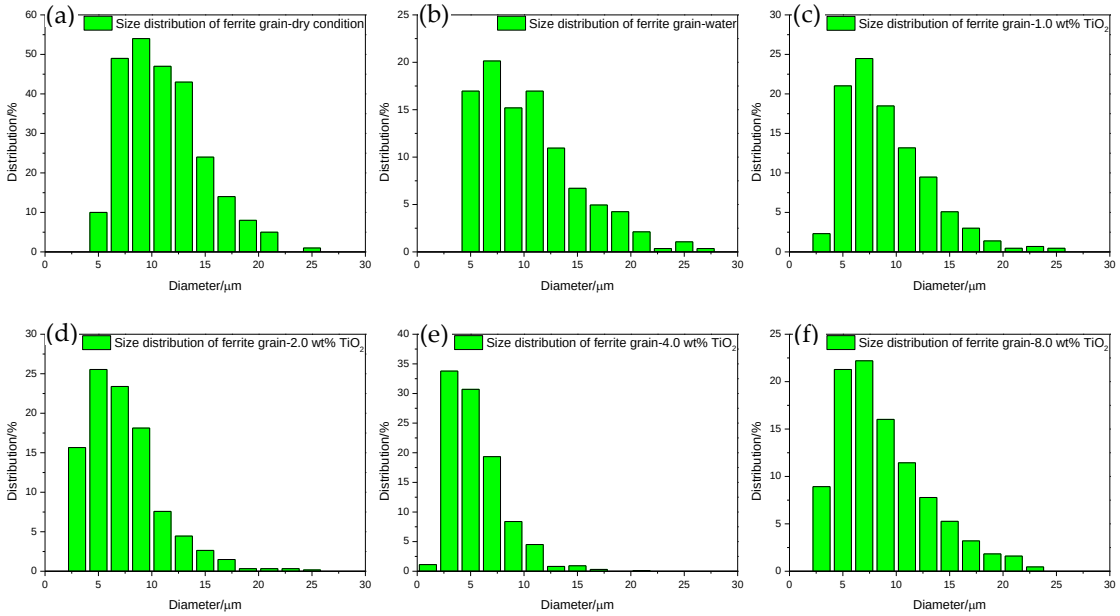

Figure 8. Size distributions of ferrite grains obtained after rolling at 850 °C under different lubrication conditions of (**a**) dry, (**b**) water, (**c**) 1.0 wt% TiO_2, (**d**) 2.0 wt% TiO_2, (**e**) 4.0 wt% TiO_2 and (**f**) 8.0 wt% TiO_2.

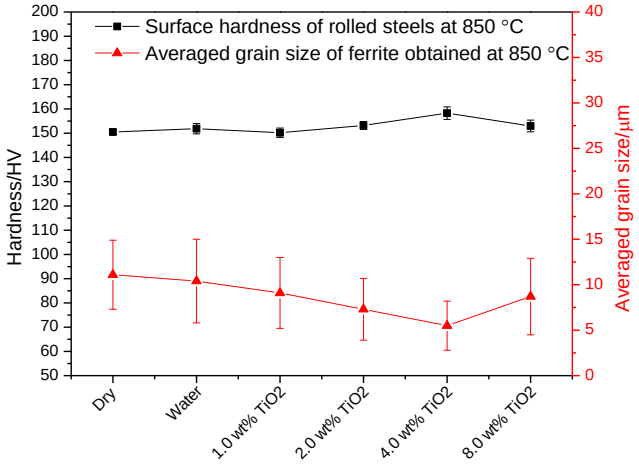

Figure 9. Surface hardness of rolled steels and averaged grain size of ferrite obtained at 850 °C under different lubrication conditions.

4. Discussion

4.1. FIB-TEM Analysis

The TEM images of FIB foil cut from the rolled steel surface, and corresponding EDS mappings of typical elements obtained under 4.0 wt% TiO_2 lubrication at 850 °C are shown in Figure 10. It can be seen from Figure 10a that there is a clear interface between the Pt-deposition layer and the oxide scale layer, and the cross section of oxide scale has considerable defects including voids and cracks. The magnified area (red zone in Figure 10a) at the interface is shown in Figure 10b. A secondary oxide scale layer with a thickness of approximately 0.06 μm exists at the top of oxide scale, which is formed due to the transfer of rolled steel from the runout table to the sealed nitrogen box. Furthermore, another layer (yellow zone) is generated underneath the secondary oxide scale layer, and the EDS mappings displayed in Figure 10e,f indicate that the layer is full of TiO_2 NPs behaving as a "lubricating film". Meanwhile, the spherical TiO_2 NPs in the lubricating film layer are able to act as bearing balls between the work roll and the workpiece, showing a "rolling effect" [25]. Both the lubricating film and the rolling effect thus contribute to decreasing the COF during the hot rolling process, which finally results in decrease of rolling force. In general, the lubrication effect on decreasing rolling force is dependent on effective amounts of well-dispersed TiO_2 NPs adhered onto the roll surface before rolling, which is determined by wettability and concentration of nanolubricant applied. In this case, the nanolubricant with better dispersibility, stronger wettability and higher concentration is more inclined to decrease rolling force to a larger extent. Many researchers have reported that the wettability of nanolubricant improves with increasing the concentration of NPs into base liquid [26–28]. Therefore, when the concentration of nano-TiO_2 is lower than 4.0 wt%, there are insufficient TiO_2 NPs left to form lubricating film and make rolling effect due to loss of nanolubricants when contacting the hot steel surface. When the concentration of nano-TiO_2 exceeds 4.0 wt% to a higher level of 8.0 wt%, instead, the rolling force varies at an opposite trend to present a higher value (see Figure 2) because of the agglomeration of TiO_2 NPs [20,21], which aggravates the friction between the work roll and the workpiece.

The white zone marked in Figure 10b, along with the EDS mappings shown in Figure 10e,f, indicates that TiO_2 NPs can also fill in the defects of steel surface during hot rolling process, exhibiting a "mending effect" [18]. The mending effect hereby facilitates the decrease of surface roughness with similar principle to that of rolling force. While the difference is that the agglomeration of TiO_2 NPs induced by 8.0 wt% nano-TiO_2 lubrication may cause even deeper scratches than those produced by 4.0 wt% nano-TiO_2 lubrication, leading to higher surface roughness. This result has been proved in our previous study by using a pin-on-disk tribological test [21]. The other reason for reducing surface roughness may be ascribed to the "polishing effect" of TiO_2 NPs [29], which helps to remove the bumps or peaks embedded in steel substrate, and thus flatten the surface of rolled steel.

The formation of oxide scale during hot rolling process involves temperature, oxygen, and water, and the possible reasons to generate different thickness under different lubrication conditions have been investigated in our previous study [22].

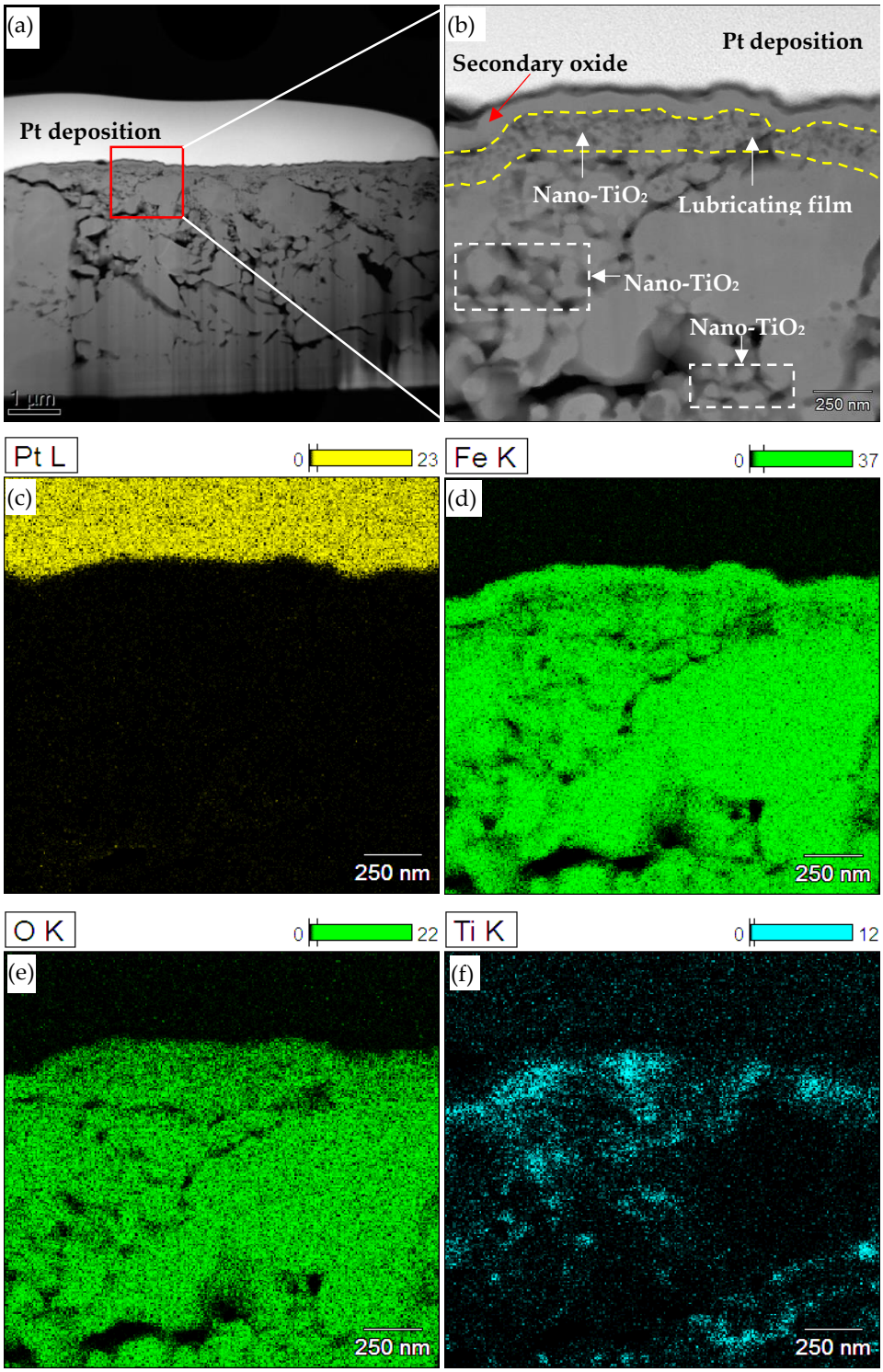

Figure 10. (**a**) Transmission electron microscope (TEM) image of focused ion beam (FIB) foil cut from rolled steel surface, (**b**) TEM image of magnified area in (**a**), and (**c**–**f**) EDS mappings of (**b**), under 4.0 wt% TiO_2 lubrication at 850 °C.

4.2. Grain Refinement Mechanism

It is well-known that controlling the nucleation and growth of grains is the fundamental method for grain refinement. In general, the ferrite grain size decreases with the increase of cooling rate and deformation of austenite in hot steel rolling [30]. Therefore, the critical influences on refining ferrite

grain in this study comprise the cooling rate of applied lubricants and the plastic deformation of the steel strip. The former is related to thermal conductivity of the effective volume of lubricants adhered onto the roll surface, while the latter refers to the thickness reduction of steel strip. Figure 11 shows the thermal conductivity of nanolubricants measured in comparison to those of water and 10 wt% glycerol. It is observed that water presents the highest thermal conductivity among all the liquids, showing a value of around 0.6 W/mK at an ambient temperature of 23 °C [31]. A possible reason is that a concentration of 10 wt% glycerol has very low thermal conductivity (0.29 W/mK) [32], which may greatly lower down the thermal conductivity of water-based solutions. The thermal conductivity of nanolubricants, however, increases with the increase of nano-TiO_2 concentration, which is consistent with the findings reported by other researchers [33–36]. Although water displays slightly higher thermal conductivity than water-based nanolubricants, it still leads to a lower cooling rate due to its poorer wettability when adhering onto the roll surface before rolling. In this case, the cooling rate of nanolubricants is higher than that of water, let alone that of dry condition, and it increases gradually with the increase of nano-TiO_2 concentration based on the variation trend of wettability reported in our previous study [22]. Thus, the ferrite grains obtained during hot rolling are supposed to be more readily refined with the application of nanolubricants, compared to those of dry condition and water. Besides, the nanolubricant containing higher nano-TiO_2 concentration is more likely to refine ferrite grains.

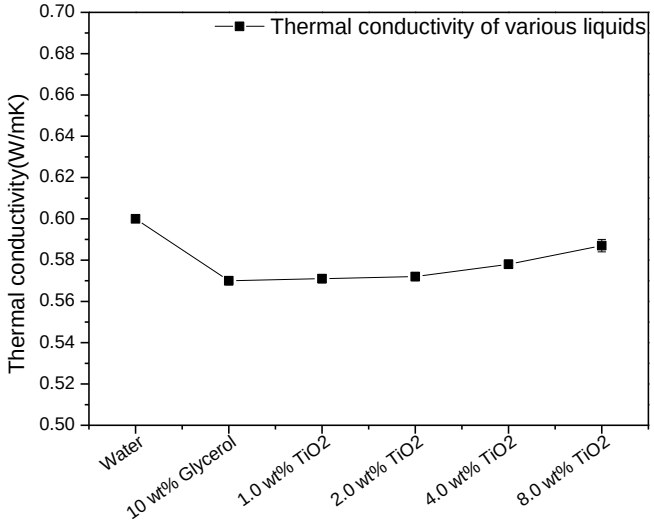

Figure 11. Thermal conductivity measured at ambient temperature as a function of various liquids.

When it comes to the effect of plastic deformation on grain refinement, the exit thickness of rolled steel needs to be considered. The relationship between exit thickness of rolled steel and rolling force is normally referred to by the Gaugemeter equation [37]:

$$h = C_0 + P/K_s \quad (1)$$

where h is the exit thickness of rolled steel, C_0 is the no-load roll gap, P is the rolling force, and K_s is the mill structural stiffness. For the rolling test conducted on the same rolling mill under the same rolling parameters, C_0 and K_s are constant. In this case, a lower rolling force is inclined to induce a thinner exit thickness of steel. The thickness values of rolled steel are shown in Figure 12, the trend of which is well matched with that obtained in Figure 2. It can be seen that the use of nanolubricant containing 4.0 wt% TiO_2 results in a rolled steel with the thinnest thickness (5.55 mm), compared to those of other lubrication conditions, presenting the greatest deformation. As a whole, the combined effects of

cooling rate together with plastic deformation induce the finest ferrite grains under nanolubrication with 4.0 wt% TiO_2, as shown in Figures 7 and 8.

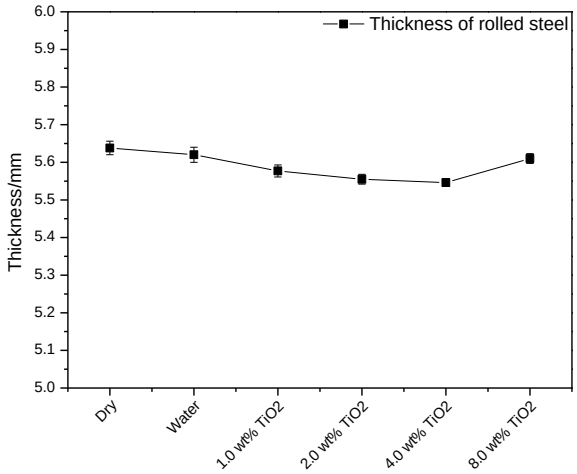

Figure 12. Final thickness of rolled steel at 850 °C under different lubrication conditions.

4.3. Illustration of Mechanisms

The lubrication and grain refinement mechanisms using nanolubricants containing nano-TiO_2 in hot steel rolling are schematically illustrated in Figure 13. When a work roll contacts a hot steel surface, the water-based nanolubricants adhered onto the roll surface are inclined to run off immediately at such a high rolling temperature of 850 °C. The retained nanolubricants simultaneously take lubrication effect in the contact area between the roll and the strip. On one hand, some of the TiO_2 NPs are able to spread over the strip surface to form a lubricating film, and some others act as ball bearings, both of which contribute to the decreased COF during hot rolling, thereby decreasing the rolling force. The lubricating film can also isolate the air, leading to a decrease of oxide scale thickness. On the other hand, a number of TiO_2 NPs are committed to removing the bumps or peaks embedded in the strip substrate, showing a polishing effect. There are also considerable TiO_2 NPs that fill in the voids and cracks of strip surface, presenting a mending effect. The polishing effect combined with the mending effect thus contributes to reducing the surface roughness of rolled steels. The most interesting point is that the nanolubricants devote themselves to refining ferrite grains obtained during hot rolling, which is ascribed to the higher thermal conductivity of the nanolubricants and larger plastic deformation of strip steels, as discussed in Section 4.2.

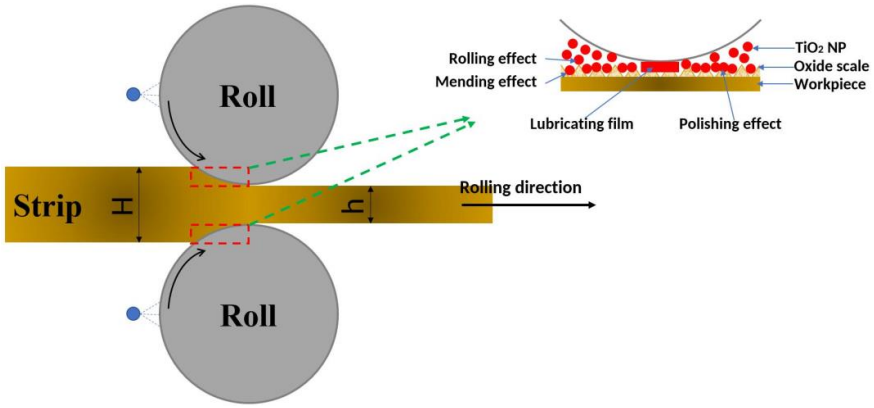

Figure 13. Schematic illustration of lubrication and grain refinement mechanisms using nanolubricants containing nano-TiO_2 in hot steel rolling at 850 °C.

5. Conclusions

In this study, the hot steel rolling tests were performed at 850 °C under dry condition, water, and water-based nanolubricants containing nano-TiO_2 concentrations varying from 1.0 to 8.0 wt%. The lubrication effects of the nanolubricants on rolling force, surface roughness, thickness of oxide scale, and microstructure were systematically investigated. The conclusions can be drawn below.

(1) The rolling force obtained under dry condition is the highest among all the tests, which can be reduced maximally by 6.8% to 564 KN when nanolubricant containing 4.0 wt% nano-TiO_2 is applied.
(2) The surface roughness of the rolled steels under dry conditions can be improved by 19.5% when using the nanolubricant with 4.0 wt% nano-TiO_2. The lubricant also produces the flattest steel surface after hot rolling.
(3) The nanolubricant containing 4.0 wt% TiO_2 produces the thinnest oxide scale, which is 43.8% thinner than that obtained under dry conditions.
(4) The use of nanolubricant containing 4.0 wt% TiO_2 leads to grain refinement to the largest extent, showing 50% finer ferrite grain size than that of dry conditions.
(5) The lubrication mechanism of water-based nanolubricants containing nano-TiO_2 in hot steel rolling is ascribed to the synergistic effect of lubricating film, rolling, polishing and mending.

Author Contributions: H.W. performed the experiments in addition to analysing the data and writing the paper; J.Z. contributed the supervision and proofreading; L.L. contributed the grain size statistics; S.H. contributed the preparation of lubricants; L.W. contributed dispersion stability of as-prepared lubricants; S.Z. contributed the supplies of steel samples; S.J. & H.H. contributed the project administration; Z.J. contributed conceptualisation and supervision.

Funding: This research was funded by Baosteel-Australia Joint Research and Development Centre (No. BA-17004) and Australian Research Council (No. LP150100591).

Acknowledgments: The authors acknowledge the financial support from Baosteel-Australia Joint Research and Development Centre (BAJC) under project of BA-17004 and Australian Research Council (ARC) under Linkage Project Program (LP150100591). The authors wish to thank Stuart Rodd, Nathan Hodges and other technicians in the workshop of SMART Infrastructure Facility at University of Wollongong (UOW) for their great supports on samples machining and operation of hot rolling mill. We also wish to thank Charlie Kong for his technical assistance and use of facilities supported by AMMRF at the Electron Microscope Unit at University of New South Wales. We also appreciate the kind assistance from David Mitchell at Electron Microscopy Centre at UOW on TEM observations. We finally would like to extend special thanks to Jun Chen at the Australian Institute for Innovative Materials at UOW for his great effort on measurement of thermal conductivity.

Conflicts of Interest: The authors declare no conflict of interest.

References

1. Wu, H. A Study of Novel Nano-Additive Water-Based Lubrication in Hot Rolling of Steels. Ph.D. Thesis, University of Wollongong, Wollongong, Australia, 2017.
2. Azushima, A.; Xue, W.D.; Yoshida, Y. Lubrication mechanism in hot rolling by newly developed simulation testing machine. *CIRP Ann.-Manuf. Technol.* **2007**, *56*, 297–300. [CrossRef]
3. Azushima, A.; Xue, W.D.; Yoshida, Y. Influence of Lubricant Factors on Coefficient of Friction and Clarification of Lubrication Mechanism in Hot Rolling. *ISIJ Int.* **2009**, *49*, 868–873. [CrossRef]
4. Matsubara, Y.; Hiruta, T.; Kimura, Y. Effect of oil film thickness on lubrication property in hot rolling. *ISIJ Int.* **2015**, *55*, 632–636. [CrossRef]
5. Williams, K. Tribology in Metal Working±New Developments, I. In Proceedings of the Mechanical Engineering Conference, London, UK, 4–6 July 1980.
6. Shirizly, A.; Lenard, J.G. The effect of lubrication on mill loads during hot rolling of low carbon steel strips. *J. Mater. Process. Technol.* **2000**, *97*, 61–68. [CrossRef]
7. Meng, Y.; Sun, J.; Wu, P.; Dong, C.; Yan, X. The Role of Nano-TiO_2 Lubricating Fluid on the Hot Rolled Surface and Metallographic Structure of SS41 Steel. *Nanomaterials* **2018**, *8*, 111. [CrossRef] [PubMed]

8. Bao, Y.; Sun, J.; Kong, L. Effects of nano-SiO_2 as water-based lubricant additive on surface qualities of strips after hot rolling. *Tribol. Int.* **2017**, *114*, 257–263. [CrossRef]
9. Spuzic, S.; Strafford, K.N.; Subramanian, C.; Savage, G. Wear of hot rolling mill rolls: An overview. *Wear* **1994**, *176*, 261–271. [CrossRef]
10. Beese, J.G. Lubrication of hot-strip-mill rolls. *Wear* **1973**, *23*, 203–208. [CrossRef]
11. Barrett, C. Influence of lubrication on through thickness texture of ferritically hot rolled interstitial free steel. *Ironmak. Steelmak.* **1999**, *26*, 393–397. [CrossRef]
12. Lenard, J.G.; Barbulovic-Nad, L. The coefficient of friction during hot rolling of low carbon steel strips. *J. Tribol.* **2002**, *124*, 840–845. [CrossRef]
13. Matsuoka, S.; Morita, M.; Furukimi, O.; Obara, T. Effect of lubrication condition on recrystallization texture of ultra-low C sheet steel hot-rolled in ferrite region. *ISIJ Int.* **1998**, *38*, 633–639. [CrossRef]
14. Yu, Y.; Lenard, J.G. Estimating the resistance to deformation of the layer of scale during hot rolling of carbon steel strips. *J. Mater. Process. Technol.* **2002**, *121*, 60–68. [CrossRef]
15. Haus, F.; German, J.; Junter, -G. Primary biodegradability of mineral base oils in relation to their chemical and physical characteristics. *Chemosphere* **2001**, *45*, 983–990. [CrossRef]
16. He, A.; Huang, S.; Yun, J.H.; Jiang, Z.; Stokes, J.; Jiao, S.; Wang, L.; Huang, H. The pH-dependent structural and tribological behaviour of aqueous graphene oxide suspensions. *Tribol. Int.* **2017**, *116*, 460–469. [CrossRef]
17. He, A.; Huang, S.; Yun, J.H.; Jiang, Z.; Stokes, J.R.; Jiao, S.; Wang, L.; Huang, H. Tribological Characteristics of Aqueous Graphene Oxide, Graphitic Carbon Nitride, and Their Mixed Suspensions. *Tribol. Lett.* **2018**, *66*, 42. [CrossRef]
18. He, A.; Huang, S.; Yun, J.H.; Wu, H.; Jiang, Z.; Stokes, J.; Jiao, S.; Wang, L.; Huang, H. Tribological Performance and Lubrication Mechanism of Alumina Nanoparticle Water-Based Suspensions in Ball-on-Three-Plate Testing. *Tribol. Lett.* **2017**, *65*, 40. [CrossRef]
19. Zhu, Z.; Sun, J.; Niu, T.; Liu, N. Experimental research on tribological performance of water-based rolling liquid containing nano-TiO_2. *Proc. Inst. Mech. Eng. Part N J. Nanoeng. Nanosyst.* **2014**, *229*, 104–109. [CrossRef]
20. Wu, H.; Zhao, J.; Cheng, X.; Xia, W.; He, A.; Yun, J.H.; Huang, S.; Wang, L.; Huang, H.; Jiao, S.; et al. Friction and wear characteristics of TiO_2 nano-additive water-based lubricant on ferritic stainless steel. *Tribol. Int.* **2018**, *117*, 24–38. [CrossRef]
21. Wu, H.; Zhao, J.; Xia, W.; Cheng, X.; He, A.; Yun, J.H.; Wang, L.; Huang, H.; Jiao, S.; Huang, L.; et al. A study of the tribological behaviour of TiO_2 nano-additive water-based lubricants. *Tribol. Int.* **2017**, *109*, 398–408. [CrossRef]
22. Wu, H.; Zhao, J.; Xia, W.; Cheng, X.; He, A.; Yun, J.H.; Wang, L.; Huang, H.; Jiao, S.; Huang, L.; et al. Analysis of TiO_2 nano-additive water-based lubricants in hot rolling of microalloyed steel. *J. Manuf. Process.* **2017**, *27*, 26–36. [CrossRef]
23. Yu, X.; Jiang, Z.; Zhao, J.; Wei, D.; Zhou, J.; Zhou, C.; Huang, Q. The role of oxide-scale microtexture on tribological behaviour in the nanoparticle lubrication of hot rolling. *Tribol. Int.* **2016**, *93*, 190–201. [CrossRef]
24. Luo, L.; Jiang, Z.; Wei, D. Influences of micro-friction on surface finish in micro deep drawing of SUS304 cups. *Wear* **2017**, *374*, 36–45. [CrossRef]
25. Chang, L.; Zhang, Z.; Breidt, C.; Friedrich, K. Tribological properties of epoxy nanocomposites - I. Enhancement of the wear resistance by nano-TiO_2 particles. *Wear* **2005**, *258*, 141–148. [CrossRef]
26. Kasraei, S.; Azarsina, M. Addition of silver nanoparticles reduces the wettability of methacrylate and silorane-based composites. *Braz. Oral Res.* **2012**, *26*, 505–510. [CrossRef] [PubMed]
27. Lim, S.; Horiuchi, H.; Nikolov, A.D.; Wasan, D. Nanofluids Alter the Surface Wettability of Solids. *Langmuir* **2015**, *31*, 5827–5835. [CrossRef] [PubMed]
28. Vafaei, S.; Borca-Tasciuc, T.; Podowski, M.Z.; Purkayastha, A.; Ramanath, G.; Ajayan, P.M. Effect of nanoparticles on sessile droplet contact angle. *Nanotechnology* **2006**, *17*, 2523. [CrossRef] [PubMed]
29. Ingole, S.; Charanpahari, A.; Kakade, A.; Umare, S.S.; Bhatt, D.V.; Menghani, J. Tribological behavior of nano TiO_2 as an additive in base oil. *Wear* **2013**, *301*, 776–785. [CrossRef]
30. Tamura, I.; Sekine, H.; Tanaka, T. *Thermomechanical Processing of High-Strength Low-Alloy Steels*; Butterworth-Heinemann: Oxford, UK, 2013.

31. Ramires, M.L.; Nieto de Castro, C.A.; Nagasaka, Y.; Nagashima, A.; Assael, M.J.; Wakeham, W.A. Standard Reference Data for the Thermal-Conductivity of Water. *J. Phys. Chem. Ref. Data* **1995**, *24*, 1377–1381. [CrossRef]
32. Tadjarodi, A.; Zabihi, F. Thermal conductivity studies of novel nanofluids based on metallic silver decorated mesoporous silica nanoparticles. *Mater. Res. Bull.* **2013**, *48*, 4150–4156. [CrossRef]
33. Ponzoni, C.; Gualtieri, M.L.; Lugli, E.; Leonelli, C.; Romagnoli, M. Stabilization and thermal conductivity of aqueous magnetite nanofluid from continuous flows hydrothermal microwave synthesis. *Mater. Lett.* **2016**, *173*, 195–198.
34. Kedzierski, M.A.; Brignoli, R.; Quine, K.T.; Brown, J.S. Viscosity, density, and thermal conductivity of aluminum oxide and zinc oxide nanolubricants. *Int. J. Refrig.* **2017**, *74*, 3–11. [CrossRef] [PubMed]
35. Özerinç, S.; Kakaç, S.; Yazıcıoğlu, A.G. Enhanced thermal conductivity of nanofluids: A state-of-the-art review. *Microfluid. Nanofluid.* **2010**, *8*, 145–170. [CrossRef]
36. Zhu, H.T.; Zhang, C.; Tang, Y.; Wang, J.; Ren, B.; Yin, Y. Preparation and thermal conductivity of suspensions of graphite nanoparticles. *Carbon* **2007**, *45*, 226–228. [CrossRef]
37. Ginzburg, V.B. *Steel-Rolling Technology: Theory and Practice*; Marcel Dekker, Inc.: New York, NY, USA, 1989; p. 791.